Efficient second-harmonic generation in silicon nitride resonant waveguide gratings

Tingyin Ning,[1,*] Henna Pietarinen,[1] Outi Hyvärinen,[2] Ravi Kumar,[1] Tommi Kaplas,[3] Martti Kauranen,[1] and Goëry Genty[1]

[1]*Department of Physics, Tampere University of Technology, P.O. Box 692, Tampere FI-33101, Finland*

[2]*Optoelectronics Research Centre, Tampere University of Technology, Tampere FI-33101, Finland*

[3]*Department of Physics and Mathematics, University of Eastern Finland, Joensuu FI-80101, Finland*

**Corresponding author: tingyin.ning@tut.fi*

Received May 30, 2012; revised August 31, 2012; accepted August 31, 2012; posted September 5, 2012 (Doc. ID 169571); published October 11, 2012

We demonstrate a thousand-fold enhancement of second-harmonic generation in an all-dielectric silicon nitride (SiN) resonant waveguide grating compared to a flat SiN film. The strong second-harmonic output measured at 532 nm results from the combination of the enhanced local fields in the nanostructure and the large second-order susceptibility of SiN. The second-harmonic conversion efficiency in the resonant structure is found to be of the order of 10^{-8}, which is significantly larger than that typically observed from plasmonic metal nanostructures. © 2012 Optical Society of America

OCIS codes: 050.1950, 050.5745, 310.6628, 190.2620.

Nonlinear frequency conversion is paramount for many applications and photonic devices. For the particular case of second-harmonic generation (SHG), the efficiency can be increased through phase matching between the interacting waves or by enhancing the local fields [1]. Phase matching is usually the preferred way for bulk materials and waveguides. On the other hand, for integrated nanophotonic applications that require materials with reduced dimensions, enhancing the local fields is generally preferred, which can be conveniently achieved, e.g., in subwavelength resonant structures [1]. Such nanoscale structures can also be seen as elementary sources of nonlinear radiation, which could be combined by optical cavities or phase-matched structures in order to further enhance the conversion efficiency.

Recent work has considered different types of structures for local-field enhancement of nonlinear processes [2–4]. Enhanced SHG in resonant nanostructures such as photonic crystals [5,6], gratings [7–9], or nanowaveguides [10,11] has been widely studied in the last decade. More recently, metal nanostructures have received increasing attention, where enhanced SHG is achieved through the strong field localization associated with the excitation of surface plasmon resonances [12–14]. However, metal nanostructures inherently suffer from significant losses that limit the SHG conversion efficiency.

All-dielectric resonant structures that are transparent both at the fundamental and SH wavelengths are promising alternatives for efficient SHG. Indeed, high-quality dielectric resonant cavities such as photonic crystals [5], microring [15], microsphere [4] or Fabry–Perot cavities [16] leading to significantly enhanced SHG have been demonstrated. Yet, it would be highly beneficial to develop nonlinear materials that are compatible with the complementary metal-oxide-semiconductor (CMOS) technology. Unfortunately, materials such as Si or GaAs [2,5] that are widely employed in nanofabrication are not transparent at visible wavelengths or only give rise to surface SHG (e.g., in SiO_2 or Si_3N_4) [15]. This severely limits the SH conversion efficiency that can be obtained in CMOS-compatible devices.

Recently, we have reported the fabrication of amorphous silicon nitride (SiN) films by plasma-enhanced chemical vapor deposition, where the particular fabrication conditions (ratio of reacting gas, SiH_4/N_2 and NH_3, temperature, gas pressure) give rise to a strong SH response [17]. The second-order susceptibility was found to be as high as 2.5 pm/V, which is comparable to that of typical nonlinear crystals.

In this Letter, we report on the large SH response in a resonant waveguide grating (RWG) made of SiN. We demonstrate the emission of SH signal enhanced by as much as a factor of 10^3 compared to a flat SiN film and with a conversion efficiency exceeding 10^{-8}. Our results show great potential for nonlinear applications of SiN RWGs as nanophotonic devices.

The SiN RWG was fabricated on a fused silica substrate and designed using rigorous coupled-wave analysis [18]. The parameters of the structure [period, duty cycle, height, and thickness of the grating, Fig. 1(a)] were optimized for coupling 1064 nm light into a p-polarized (TM) waveguide mode at a resonant incident angle of about 16.33°. The RWG with dimensions 4×4 mm^2 [see Fig. 1(b)] was manufactured using standard nanofabrication techniques. Specifically, a master plate was first patterned by electron-beam lithography and then transferred onto 800 nm thick SiN films by UV nanoimprint lithography and etching. A scanning electron microscope (SEM) image of the grating is shown in Fig. 1(c). The grating period is 580 nm with 0.59 duty-cycle for SiN. The groove depth and the thickness of the SiN waveguide layer are $H_g \sim 676$ nm and $W_g \sim 124$ nm, respectively. The calculated out-of-plane magnetic field is shown in Fig. 1(d). The numerical simulation predicts an enhancement of the local field amplitude by a factor of about 30 in the grating-waveguide cavity (in comparison with the incident plane wave), which is much larger than the field enhancement for SiO_2/TiO_2 gratings [7,8]

The linear transmission and SHG efficiency were measured using setups similar to those described in [7,8]. The

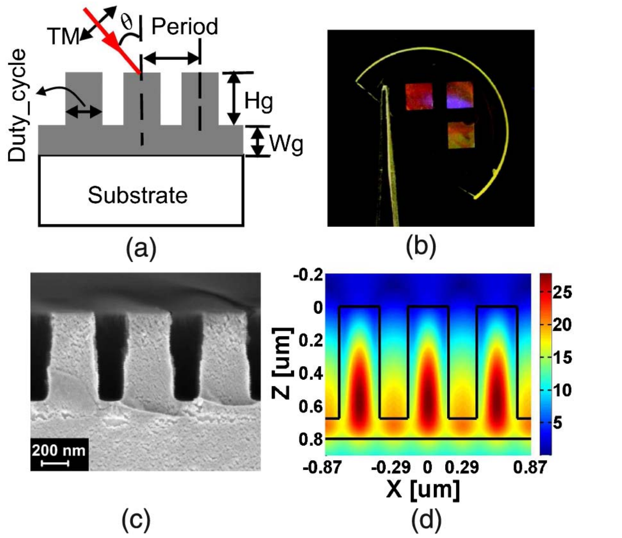

Fig. 1. (Color online) (a) Schematic of the RWG structure. (b) Photograph of the RWG with dimension $4 \times 4\ \mathrm{mm}^2$ on a fused silica substrate. (c) SEM image of the SiN RWG. (d) Calculated amplitude of the out-of-plane magnetic field component in the periodic RWG structure at resonant conditions.

sample was illuminated with 70 ps pulses from a Nd:YAG laser operating at 1064 nm wavelength with a repetition rate of 1 kHz. The beam was collimated to 1 mm diameter so as to minimize the divergence and thus enable efficient coupling into the resonant waveguide mode. The exact resonance angle was determined by recording the intensity of the transmitted fundamental beam while varying the angle of incidence. The results in Fig. 2 clearly show a relatively sharp resonance for an incidence angle of 17.93°. The additional features are related to Fabry–Perot resonances of the 1 mm thick substrate. The theoretical transmission including the Fabry–Perot resonances of the substrate is also shown and it is in good qualitative agreement with the experiment. Nevertheless, we observe a slight shift in the resonance angle and the resonance bandwidth is larger than predicted for the ideal design (0.37° versus 0.22°). We attribute these discrepancies to small imperfections and inhomogeneities in the nanostructure. The insertion loss of the device on resonance at 1064 nm was measured to be 1.3 dB.

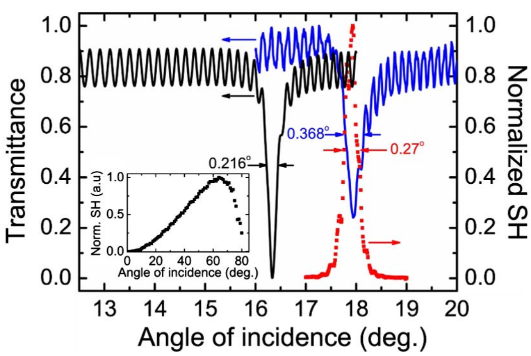

Fig. 2. (Color online) Simulated (blue) and experimentally measured (black) angular dependence of the RWG linear transmittance. The normalized SHG from the RWG is shown as red squares and the inset shows the normalized SHG from the reference SiN film.

The SHG measurements performed for p-polarized fundamental and SH light as a function of incidence angle exhibit clear resonant enhancement with a narrow peak centered at the resonance angle of the linear transmission. The SHG acceptance angle was found to be 0.27°, which is slightly less than that of the fundamental resonance. Varying the polarization state of the fundamental beam with a half-wave plate confirmed that p-polarized fundamental light indeed leads to the strongest SH signal (also p-polarized) at the resonance angle. In contrast, s-polarized fundamental light did not produce any detectable SH signal. These findings are consistent both with SHG in SiN films possessing in-plane isotropy and broken centrosymmetry along the surface normal, and with the numerical simulations of enhanced local fields in RWGs [7,8].

In order to quantify the SHG enhancement factor for the RWG, we have compared the SH signal from the grating with that from a planar SiN film. The SiN films for the RWG and the reference were prepared under identical conditions as described in [17] and with the same thickness of 800 nm. We conducted the SH measurement for the RWG and reference separately but using the same setup. The SHG intensity from the reference as a function of incidence angle was recorded for p-polarized fundamental light. The maximum SH signal was found at the incidence angle of $\sim 65^{\circ}$ (see inset in Fig. 2), and it is this maximum value that was used as reference for the RWG. Specifically, comparing the intensity of the SH signal from the RWG at the resonance angle, we estimate the enhancement factor arising from the resonant grating to be approximately 1000. Because the SHG signal from the SiN film is itself three orders of magnitude larger than that from a planar fused silica surface [17], we can further estimate the SH signal generated by the SiN RWG to be 10^6 times larger than for a typical dielectric surface.

In order to obtain the absolute SHG power and determine the SHG conversion efficiency from the SiN RWG at the resonance angle, the photomultiplier tube (PMT) used to detetct SH light was calibrated at the 532 nm SH wavelength. For this purpose, we used a potassium titanyl phosphate (KTP) crystal that generates SH light measurable with a calibrated silicon detector. To avoid saturation, the SH signal from the KTP crystal was attenuated before the PMT with calibrated neutral density filters. Accounting for the filters' attenuation, a linear relation between the measured value from the PMT and actual SHG power could be deduced and the SH signal from the RWG converted into power units. The results are shown in Fig. 3 in a log-log scale for increasing incident power up to 15 mW, which is the limit of our laser for a 1 mm collimated beam. The conversion efficiency for 10 mW input power is 1.5×10^{-8}, which is consistent with our previously determined $\chi^{(2)}$ for SiN films [17] and with the insertion loss of the structure. Remarkably, the large conversion efficiency in the RWG structure could be readily seen with the naked eye from a white screen behind the sample (inset in Fig. 3). The damage threshold in terms of input average power was estimated to be $\sim$100 mW [19], implying that the SHG conversion efficiency in the RWG could potentially reach as much as 1.5×10^{-7} on resonance.

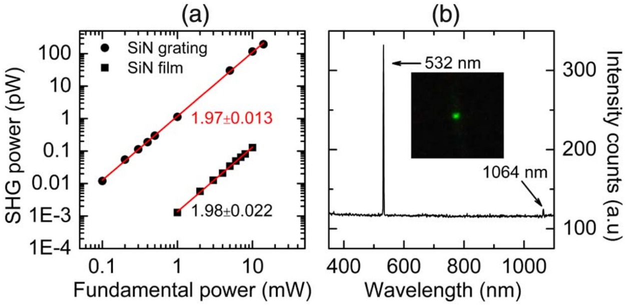

Fig. 3. (Color online) (a) Measured SH power versus fundamental laser power on a log-log scale. The squares represent results for the reference film and the circles for the RWG. The solid lines show a linear fit with a slope of approximately 2. (b) Experimental spectra of the fundamental and SH signals (measured after a short-pass filter). Inset: photograph of the SHG observed on a white screen and taken by a digital camera for a 40 mW fundamental power and 3 mm collimated beam.

Significantly, the maximum conversion efficiency from the SiN RWG is of the same order of magnitude as that recently reported from asymmetric bowtie aperture arrays (1.4×10^{-8}) [14], and one and three orders of magnitude larger than from gold nanocups (1.8×10^{-9}) [12] and plasmonic electric field-induced SHG (5.7×10^{-11}) [13], respectively. Similarly to the SiN RWG reported here, strong SHG from these nanostructures was ascribed to the enhanced local fields at the resonance condition, which is commonly believed to be the most promising way to enhance nonlinear processes at the nanoscale.

In conclusion, we have demonstrated efficient SHG from a RWG made of all CMOS-compatible materials. The conversion efficiency was measured to be of the order of 10^{-8} which is enhanced by a factor of 10^3 compared to a flat SiN film under optimal conditions. The conversion efficiency is yet lower than that recently observed in a Si_3N_4 ring resonator [15] (10^{-4} for 315 mW average pump power) but obtained under multimode phase-matching and resonant conditions, and with a much larger input intensity. However, we anticipate that similar efficiency could be obtained in a RWG where both the fundamental and SH waves are simultaneously resonant and/or where multimode phase-matching is achieved in the waveguide.

This work is supported by the Academy of Finland (Grant No. 134980).

References and Notes

1. L. Novotny and B. Hecht, *Principles of Nano-Optics* (Cambridge, 2006).
2. M. Soljacic and J. D. Joannopoulos, Nat. Mater. **3**, 2011 (2004).
3. J. S. Levy, A. Gondarenko, M. A. Foster, A. C. Turner-Foster, A. L. Gaeta, and M. Lipson, Nat. Photonics **4**, 37 (2010).
4. J. L. Dominguez-Juarez, G. Kozyreff, and J. martorell, Nat. Commun. **2**, 254 (2011).
5. J. P. Mondia, H. M. van Driel, W. Jiang, A. R. Cowan, and J. F. Young, Opt. Lett. **28**, 2500 (2003).
6. A. M. Malvezzi, G. Vecchi, M. Patrini, G. Guizzetti, L. C. Andreani, F. Romanato, L. Businaro, E. Di Fabrizio, A. Passaseo, and M. De Vittorio, Phy. Rev. B **68**, 161306(R) (2003).
7. M. Siltanen, S. Leivo, P. Voima, M. Kauranen, P. Karvinen, P. Vahimaa, and M. Kuittinen, Appl. Phys. Lett. **91**, 111109 (2007).
8. A. Saari, G. Genty, M. Siltanen, P. Karvinen, P. Vahimaa, M. Kuittinen, and M. Kauranen, Opt. Express **18**, 12298 (2010).
9. D. de Ceglia, G. DAguanno, N. Mattiucci, M. A. Vincenti, and M. Scalora, Opt. Lett. **36**, 704 (2011).
10. L. Scaccabarozzi, M. M. Fejer, Y. Huo, S. Fan, X. Yu, and J. S. Harris, Opt. Lett. **31**, 3626 (2006).
11. Z. Qi, T. Li, and S. N. Zhu, J. Phys. D **41**, 025109 (2008).
12. Y. Zhang, N. K. Grady, C. Ayala-Orozco, and N. J. Halas, Nano Lett. **11**, 5519 (2011).
13. W. Cai, A. P. Vasudev, and M. L. Brongersma, Science **333**, 1720 (2011).
14. S. Park, J. W. Hahn, and J. Yong Lee, Opt. Express **20**, 4856 (2012).
15. J. S. Levy, M. A. Foster, A. L. Gaeta, and M. Lipson, Opt. Express **19**, 11415 (2011).
16. S. Lettieri, S. Di. Finizio, P. Maddalena, V. Ballarini, and F. Giorgis, Appl. Phys. Lett. **81**, 4706 (2002).
17. T. Ning, H. Pietarinen, O. Hyvrinen, J. Simonen, G. Genty, and M. Kauranen, Appl. Phys. Lett. **100**, 161902 (2012).
18. M. G. Moharam, E. B. Grann, D. A. Pommet, and T. K. Gaylord, J. Opt. Soc. Am. A **12**, 1068 (1995).
19. In fact, the damage threshold was measured in a focused beam configuration by increasing gradually the input laser power and monitoring the SHG signal, and it was then converted into an equivalent power for a collimated beam of 1 mm.